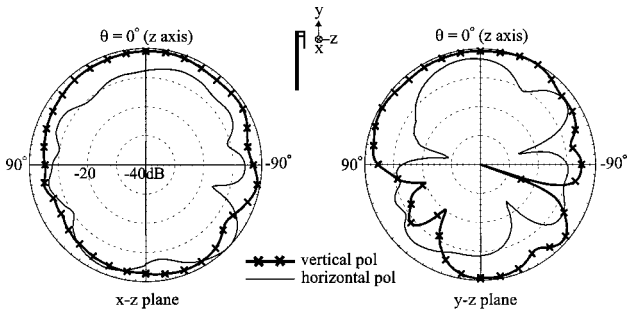

Figure 5 Measured radiation patterns for the proposed antenna at 1790 MHz

Good radiation characteristics for the two operating frequencies have also been observed.

REFERENCES

1. Z.D. Liu, P.S. Hall, and D. Wake, Dual-frequency planar inverted-F antenna, IEEE Trans Antennas Propagat 45 (1997), 1451–1458.
2. S. Tarvas and A. Isohatala, An internal dual-band mobile phone antenna, 2000 IEEE Antennas Propagat Soc Int Symp Dig, pp. 266–269.
3. C.R. Rowell and R.D. Murch, A compact PIFA suitable for dual-frequency 900/1800-MHz operation, IEEE Trans Antennas Propagat 46 (1998), 596–598.
4. C.T.P. Song, P.S. Hall, H. Ghafouri-Shiraz, and D. Wake, Triple band planar inverted F antennas for handheld devices, Electron Lett 36 (2000), 112–114.
5. P. Salonen, M. Keskilammi, and M. Kivikoski, New slot configurations for dual-band planar inverted-F antenna, Microwave Opt Technol Lett 28 (2001), 293–298.
6. W.P. Dou and Y.W.M. Chia, Novel meandered planar inverted-F antenna for triple-frequency operation, Microwave Opt Technol Lett 27 (2000), 58–60.

SIMULATION OF BEAM PROPAGATION IN SECOND-ORDER NONLINEAR OPTICAL MEDIA

K. M. Furati,[1] M. A. Alsunaidi,[2] and H. M. Masoudi[2]
[1] Department of Mathematical Sciences
King Fahd University of Petroleum and Minerals
Dhahran 31261, Saudi Arabia
[2] Department of Electrical Engineering
King Fahd University of Petroleum and Minerals
Dhahran 31261, Saudi Arabia

Received 21 August 2001

ABSTRACT: *Second-order nonlinearity in optical media acts as a source for harmonics generation. We set up a time-domain model that accounts not only for the second harmonic, but also for the higher harmonics that are induced by a beam propagation. The model is solved numerically using a second-order explicit scheme based on the exact solution of the nonlinear difference equation. The power spectrum of the generated harmonics is also presented.* © 2002 John Wiley & Sons, Inc. Microwave Opt Technol Lett 32: 312–316, 2002.

Key words: *nonlinear optics; finite difference; time domain; harmonics*
DOI 10.1002 / mop.10164

Contract grant sponsor: King Fahd University of Petroleum and Minerals, Dhahran, Saudi Arabia

1. INTRODUCTION

Second-order nonlinearity in optical media has extensive applications that are based on frequency conversion. Such conversion can serve as a laser source that has potential applications in data storage and display technology.

Modeling the second-order nonlinear effects has increasing importance in designing optical devices. There have been enormous attempts to model such effects using frequency-domain representation; see, for example, [3–5, 7–9]. Many approximations and assumptions were utilized for the analytical and numerical treatment of such models. In particular, systems are confined in advance to particular frequencies.

Alsunaidi, Masoudi, and Arnold [1] proposed a time-domain model for second-harmonic generation (SHG) in optical waveguides. However, the simulation is based on a simplified version of the model, and thus significant contributions of the nonlinearity were not accounted for.

Furati, Alsunaidi, and Masoudi [6] presented and validated an algorithm that avoids the simplifying assumptions on the time derivatives imposed in [1]. Doing so, the time-domain numerical solution preserves the characteristics of the nonlinearity as well as coupling, and can be extended to arbitrary input waveform conditions such as pulsed optical beams. By considering the phase-matched propagation of a field of power 10^7 V/m, the model is excellent in simulating the evolution of the SHG since the effects of the higher harmonics are negligible.

In this paper, we extend the model in [6, 1] to study the generation of higher harmonics in second-order nonlinear optical media. The model is rederived by distinguishing between all even and odd frequencies generated due to the nonlinear polarization, which couples all harmonic fields. We derive a second-order explicit finite-difference scheme for the coupled nonlinear wave equations, and analyze the uniqueness of the numerical solution.

Next, we set up and scale the mathematical model. Then, we discretize the model, and analyze the solutions of the discrete equations. Finally, we run the algorithm for the planar-wave case, and analyze the spectrum of the solution.

2. MATHEMATICAL MODEL

The beam propagation in a second-order nonlinear medium is described by

$$c^2 \Delta E = n^2 \partial_{tt} E + \partial_{tt} P$$
$$P = \chi^{(2)} EE$$

where E and P are the electric field and nonlinear polarization, respectively. n is the material refractive index, and c is the speed of light. $\chi^{(2)}$ is the second-order susceptibility [2, 11]. The operator Δ is the spatial Laplacian.

We are interested in processes in which a beam of frequency ω is incident upon the medium that occupies the half space $z \geq 0$, and the beam is normal to the plane $z = 0$. As the beam propagates into the medium, the nonlinear polarization term generates the higher harmonics $2\omega, 3\omega, \ldots$. Because of the differentiation, the zero-frequency field is not generated.

Let E_k denote the field of frequency $k\omega$. Define the fields

$$E_o = \sum_{k=1}^{\infty} E_{2k-1}, \qquad E_e = \sum_{k=1}^{\infty} E_{2k}.$$

We refer to E_o and E_e as odd- and even-harmonics fields.

We decompose the total field into

$$E = E_e + E_o$$

and, as in [2, 11], we assume that the nonlinear polarization is a result of the interaction of two odd-harmonics fields with an even-harmonics field:

$$P = \chi^{(2)}(E_o E_o + 2E_o E_e).$$

We assume that $\chi^{(2)}$ is frequency independent.

Note that the term $E_o E_o$ generates even frequencies, while the term $E_o E_e$ generates odd frequencies. By grouping terms of the same frequency type, the propagation equation can be split into

$$\begin{aligned} c^2 \Delta E_o &= n_o^2 \partial_{tt} E_o + 2\chi^{(2)} \partial_{tt}(E_o E_e) \\ c^2 \Delta E_e &= n_e^2 \partial_{tt} E_e + \chi^{(2)} \partial_{tt}(E_o E_o). \end{aligned} \tag{1}$$

We assume that the medium is initially unexcited, and consider incident waves of the form

$$E_{\text{in}}(x, y, z = 0, t) = A(x, y)\cos(\omega t + \phi)$$

where ϕ is the phase and $A(x, y)$ is in $L^2(R^2)$, the space of square integrable functions. Such a sinusoidal input is used in typical practical problems [1, 9].

Thus, we can write the initial and boundary conditions for (1) as

$$E_a(x, y, z, 0) = 0, \qquad \partial_t E_a(x, y, z, 0) = 0, \qquad a = e, o$$

and

$$E_o(x, y, 0, t) = A(x, y)\cos(\omega t + \phi), \qquad E_e(x, y, 0, t) = 0$$

respectively.

3. SCALING

Let I denote the energy applied to the boundary, and let it be defined by the L^2 norm of $A(x, y)$. Let λ be the wavelength $2\pi c/\omega$. If we apply the change of variables

$$x' = x/\lambda, \qquad y' = y/\lambda, \qquad z' = z/\lambda, \qquad t' = \frac{ct}{n_o \lambda}$$

$$E_a' = E_a/I, \qquad A' = A/I, \qquad \omega' = \frac{\omega n_o \lambda}{c}$$

and then remove the primes, we get the dimensionless initial-boundary value problem:

$$\begin{aligned} \Delta E_o &= \partial_{tt} E_o + 2\varepsilon \partial_{tt}(E_o E_e) \\ \Delta E_e &= r\partial_{tt} E_e + \varepsilon \partial_{tt}(E_o E_o) \\ E_o(x, y, 0, t) &= A(x, y)\cos(\omega t + \phi), \qquad E_e(x, y, 0, t) = 0 \\ E_a(x, y, z, 0) &= 0, \qquad \partial_t E_a(x, y, z, 0) = 0, \qquad a = e, o \end{aligned} \tag{2}$$

where $r = n_e^2/n_o^2$ and $\varepsilon = \chi^{(2)} I/n_o^2$.

Note that, when $r = 1$ (phase matching), all of the frequencies will propagate at the same speed.

4. DISCRETIZATION

The system (2) is fully nonlinear and coupled. Using central differencing, the finite-difference equations are also nonlinear; however, they can be decoupled.

We discretize (2) by replacing each derivative by its central difference approximation. We consider a uniform discretization of time by a time step of size dt. Let $\mathscr{E}_a^n$, $a = e, o$, denote the approximation of E_a at the time $t = ndt$.

Using these approximations, we obtain the finite-difference equations:

$$\begin{aligned} \delta^n \mathscr{E}_o = {} & \frac{\mathscr{E}_o^{n+1} - 2\mathscr{E}_o^n + \mathscr{E}_o^{n-1}}{dt^2} \\ & + 2\varepsilon \frac{\mathscr{E}_o^{n+1}\mathscr{E}_e^{n+1} - 2\mathscr{E}_o^n \mathscr{E}_e^n + \mathscr{E}_o^{n-1}\mathscr{E}_e^{n-1}}{dt^2} \end{aligned} \tag{3}$$

$$\begin{aligned} \delta^n \mathscr{E}_e = {} & r\frac{\mathscr{E}_e^{n+1} - 2\mathscr{E}_e^n + \mathscr{E}_e^{n-1}}{dt^2} \\ & + \varepsilon \frac{\mathscr{E}_o^{n+1}\mathscr{E}_o^{n+1} - 2\mathscr{E}_o^n \mathscr{E}_o^n + \mathscr{E}_o^{n-1}\mathscr{E}_o^{n-1}}{dt^2} \end{aligned} \tag{4}$$

where $\delta^n \mathscr{E}_a$ denotes the central difference approximation of ΔE_a at $t = ndt$.

Using (4) to eliminate $\mathscr{E}_e^{n+1}$ from (3), we get the cubic polynomial in $\mathscr{E}_o^{n+1}$:

$$(\mathscr{E}_o^{n+1})^3 + b_n \mathscr{E}_o^{n+1} + c_n = 0 \tag{5}$$

with the coefficients

$$\begin{aligned} b_n &= -\frac{r}{2\varepsilon^2} - \frac{r l_e^n}{\varepsilon} - \sigma_{oo}^n \\ c_n &= \frac{r l_o^n}{2\epsilon^2} + \frac{r\sigma_{oe}^n}{\varepsilon} \end{aligned} \tag{6}$$

where

$$l_a^n = 2\mathscr{E}_a^n - \mathscr{E}_a^{n-1} + dt^2 \delta^n \mathscr{E}_a, \qquad \sigma_{ab}^n = \mathscr{E}_a^n \mathscr{E}_b^n - 2\mathscr{E}_a^{n-1}\mathscr{E}_b^{n-1}, \quad a = o, e.$$

If we let

$$Q_n = \frac{-b_n}{3}, \qquad R_n = \frac{c_n}{2}$$

then we have

$$\begin{aligned} 6\varepsilon^2 Q_n &= r + 2r\varepsilon l_e^n + 2\varepsilon^2 \sigma_{oo}^n \\ &\geq r - 2r\varepsilon - 6\varepsilon^2 = (1 - 2\varepsilon)r - 6\varepsilon^2 \end{aligned}$$

and

$$\frac{R_n^2}{Q_n^3} = \frac{27 r^2 \varepsilon^2 [l_o^n + 2\varepsilon\sigma_{oe}^n]^2}{2[r + 2\varepsilon r l_e^n + 2\varepsilon^2 \sigma_{oo}^n]^3}. \tag{7}$$

Note that, for sufficiently small ε, Q_n is positive, and the ratio R_n^2/Q_n^3 is less than 1. It follows that $D_n = R_n^2 - Q_n^3 < 0$, and as a result, the polynomial (5) has the following three real solutions (cf. [10, pp. 178–180]):

$$y_i^{n+1} = -2\sqrt{Q_n}\cos\Theta_{ni}, \qquad i = 1, 2, 3$$

where

$$\Theta_{n1} = \frac{\theta_n - 2\pi}{3}, \qquad \Theta_{n2} = \frac{\theta_n + 2\pi}{3}, \qquad \Theta_{n3} = \frac{\theta_n}{3}$$

and

$$\theta_n = \arccos\left(R_n/\sqrt{Q_n^3}\right).$$

5. UNIQUENESS OF THE NUMERICAL SOLUTION

Note that $\lim_{\varepsilon\to 0}\theta_n = \pi/2$ since, from (7), $\lim_{\varepsilon\to 0}(R_n^2/Q_n^3) = 0$. Consequently, we have

$$\lim_{\varepsilon\to 0}\Theta_{n1} = -\frac{\pi}{2}, \qquad \lim_{\varepsilon\to 0}\Theta_{n2} = \frac{5\pi}{6}, \qquad \lim_{\varepsilon\to 0}\Theta_{n3} = \frac{\pi}{6}.$$

This implies that, for $i = 2, 3$,

$$\lim_{\varepsilon\to 0} y_i^{n+1} = \infty$$

since $\lim_{\varepsilon\to 0}\cos\Theta_{ni} \neq 0$, and $\lim_{\varepsilon\to 0} Q_n = \infty$.

On the other hand, $\lim_{\varepsilon\to 0}\cos\Theta_{n1} = 0$, and thus, $\lim_{\varepsilon\to 0} y_1^{n+1}$ is an undetermined form. By applying L'Hopitals rule, we get

$$\lim_{\varepsilon\to 0} y_1^{n+1} = -2\lim_{\varepsilon\to 0}\frac{\cos\Theta_{n1}}{Q_n^{-3/2}} = -\frac{4}{3}\lim_{\varepsilon\to 0}\left(\theta'_n \sin\Theta_{n1}\frac{Q_n^{3/2}}{Q'_n}\right) = l_o^n$$

since

$$\lim_{\varepsilon\to 0}\sin\Theta_{n1} = -1, \qquad \lim_{\varepsilon\to 0}\theta'_n = -\frac{3\sqrt{6}}{2\sqrt{r}}l_o^n,$$

$$\lim_{\varepsilon\to 0}\frac{Q_n^{3/2}}{Q'_n} = -\frac{\sqrt{r}}{2\sqrt{6}}.$$

Accordingly, we only admit y_1^{n+1} as the solution of (5) since it is the only one that converges to the solution of the linear equation. Therefore, for the numerical solution, we have the formula

$$\mathscr{E}_o^{n+1} = -2\sqrt{Q_n}\cos\left(\frac{\theta_n - 2\pi}{3}\right). \tag{8}$$

Once $\mathscr{E}_o^{n+1}$ is calculated, $\mathscr{E}_e^{n+1}$ is calculated explicitly from (4).

The time step can be chosen based on the CFL condition. For example, one can use a uniform time step corresponding to the maximum of the propagation speeds:

$$\left\{\frac{1}{\sqrt{1-2\varepsilon}}, \qquad \frac{1}{\sqrt{r}}\right\}.$$

6. NUMERICAL EXAMPLE

To demonstrate the validity of the derivation and the predicted behavior, we assume the incident beam to be a plane wave of compact support and the propagation in the medium to be along the positive z-direction only. In this case, the model (2) can be considered as one dimensional.

As an example, consider the boundary condition

$$E_o(0, t) = \sin 2\pi t.$$

In this case, we have $\omega = 2\pi$, and the generated frequencies should be $2, 3, 4, \ldots$. We run the algorithm (8) for $r = 1$, and $\varepsilon = 0.005$. We use the space resolution $dz = 0.01$ and time step $dt = 0.009$.

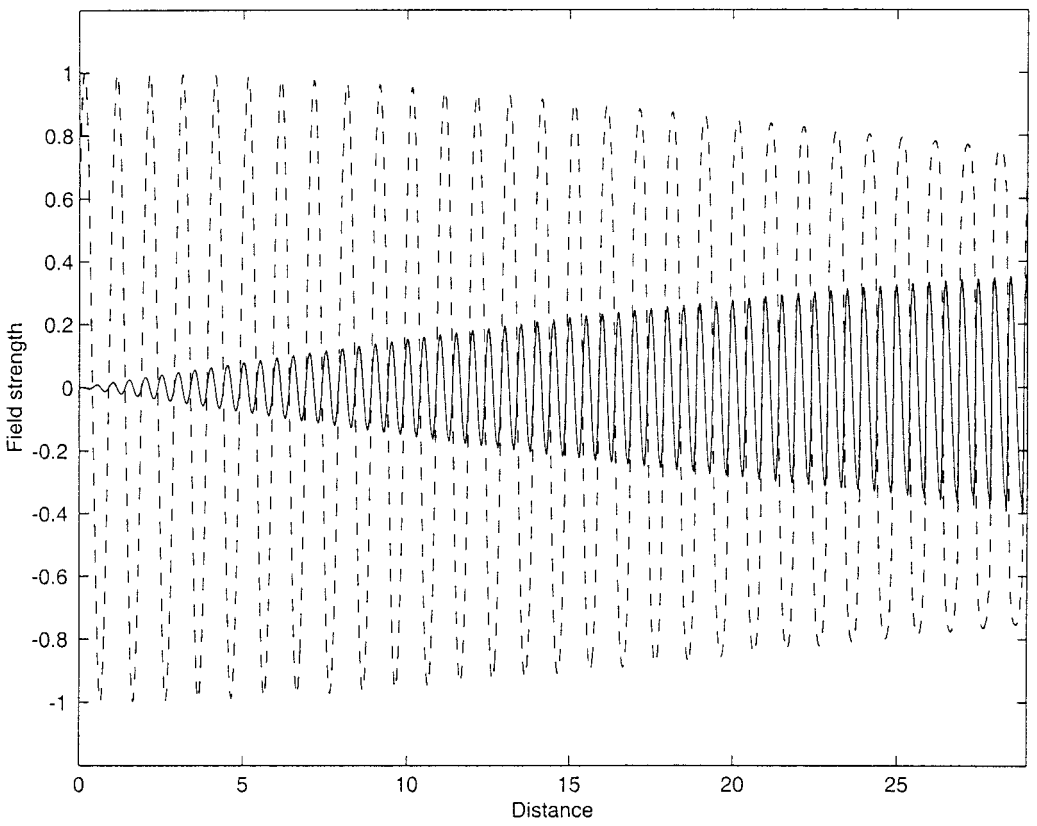

Figure 1 Wave propagation at the normalized time $t = 41.4$

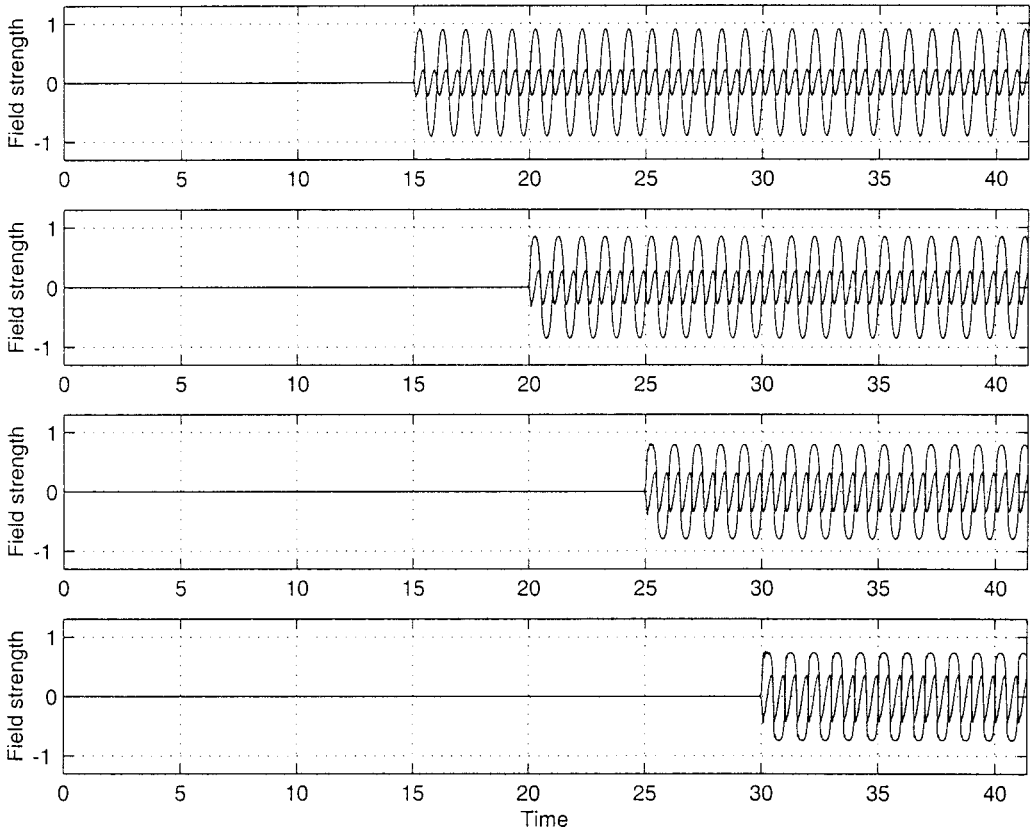

Figure 2 Time evolution of the fields at the normalized distances $z = 15, 20, 25, 30$

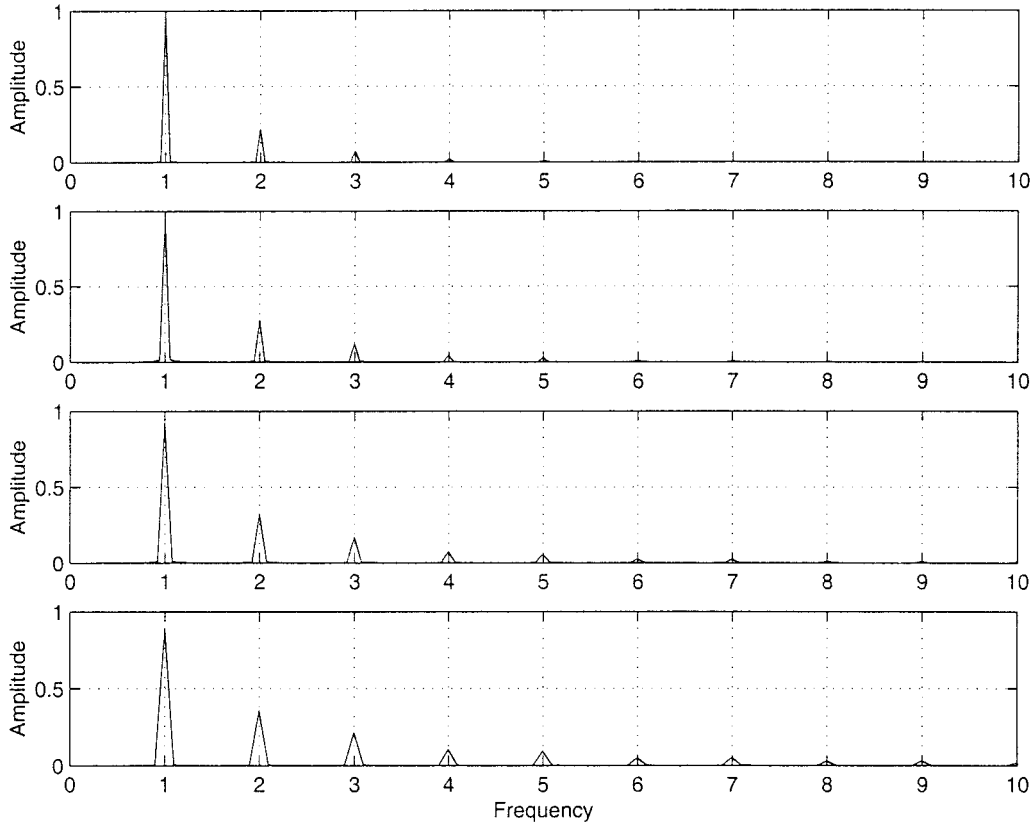

Figure 3 Time spectrum of the fields at the normalized distances $z = 15, 20, 25, 30$

Figure 1 shows the wave propagation at $t = 41.4$. The dashed and solid curves are the graphs of the numerical approximations of E_o and E_e, respectively. The energy exchange to the generated harmonics increases with the traveling distance.

Figure 2 shows the time evolution at the points $z = 15, 20, 25, 30$. The curve of larger amplitude is the graph of the odd-harmonic field numerical values. The other one is the graph of the even-harmonic field numerical values.

Figure 3 show the spectrum at the above-mentioned distances. The spectrum of the odd-harmonic field produces peaks at the frequencies $\omega = 1, 3, 5, \ldots$. The spectrum of the even-harmonic field produces peaks at the frequencies $\omega = 2, 4, 6, \ldots$.

These graphs show that, as the fields propagate inside the medium, higher harmonics are generated, and more energy is exchanged to these harmonics.

7. CONCLUSION

The mathematical model considered in this work can be used to describe more accurately the frequency conversion process that takes place in second-order nonlinear optical media. The finite-difference scheme derived retains all of the nonlinear effects, while maintaining the second-order accuracy. By applying the above model and method to practical optical structures, one can better understand the nonlinear effects that have been observed experimentally.

REFERENCES

1. M.A. Alsunaidi, H.M. Masoudi, and J.M. Arnold, A time-domain algorithm for the analysis of second harmonic generation in nonlinear optical structures, IEEE Photon Technol Lett 12 (2000), 395–397.
2. R.W. Boyd, Nonlinear optics, Academic, New York, 1992.
3. H.-F. Chou, C.-F. Lin, and G.-C. Wang, An iterative finite difference beam propagation method for modeling second-order nonlinear effects in optical waveguides, J Lightwave Technol 16 (1998), 1686–1693.
4. M. Feit and J. Fleck, Light propagation in graded-index optical fibers, Appl Opt 17 (1978), 3990–3998.
5. M. Fejer and G. Magel, Quasi-phase matched second harmonic generation: Tuning and tolerance, IEEE J Quantum Electron 28 (1992), 2631–2654.
6. K.M. Furati, M.A. Alsunaidi, and H.M. Masoudi, An explicit finite difference scheme for wave propagation in nonlinear optical structures, Appl Math Lett 14 (2001), 297–302.
7. V. Hermansson and D. Yevick, A propagation beam method analysis of nonlinear effects in optical waveguides, Opt Quantum Electron 16 (1984), 525–534.
8. G.J. Krijnen, H.J. Hoekstra, and P.V. Lambeck (Editors), BPM simulations of integrated optic structures containing second order nonlinearity, European Conf Integrated Opt, 1993, pp. 5-4–5-5.
9. H.M. Masoudi and J.M. Arnold, Parallel beam propagation method for the analysis of second harmonic generation, IEEE Photon Technol Lett 7 (1995), 400–402.
10. W.H. Press, B.P. Flannery, S.A. Teukolsky, and W.T. Vetterling, Numerical recipes in FORTRAN: The art of scientific computing, Cambridge University Press, Cambridge, England, 1992, 2nd ed.
11. A. Yariv, Optical electronics, Saunders College Publishing, Philadelphia, PA, 1991.

A GAIN-CLAMPED ERBIUM-DOPED FIBER AMPLIFIER (GC – EDFA) FOR WDM OPTICAL PACKET-SWITCHING SYSTEM

C. R. Yang,[1] H. Y. Hwang,[1] and H. H. Hong[1]
[1] Optical Packet Switch Team
Electronics and Telecommunications Research Institute
Kajong-Dong 161, Yusong-Gu, Taejon 305-350, Korea

Received 29 August 2001

ABSTRACT: *The use of dual-stage gain-clamped erbium-doped fiber amplifier (GC–EDFA) having a pump laser diode and 16-channel wavelength-division multiplexing (WDM) of 0.8 nm spacing in the C-band of 1545–1560 nm wavelength was demonstrated in a burst packet-mode optical switching system through an experimental setup.*
© 2002 John Wiley & Sons, Inc. Microwave Opt Technol Lett 32: 316–319, 2002.

Key words: *erbium-doped fiber amplifier; packet-switching system; power transient; wavelength-division multiplexing*
DOI 10.1002 / mop.10165

I. INTRODUCTION

In case some channels are added/dropped from a WDM network due to any reconfiguration or any partial failure of the network, the input signal, which is transmitted to an erbium-doped fiber amplifier (EDFA) from the WDM network, is varied, which in turn causes an undesirable power transient or output variation [1] to take place in the surviving channels. Therefore, the WDM packet-mode optical switching system, where the traffic input condition is varied in burst, is required to have an amplifier having a characteristic of amplifying the signal constantly irrespective of the transient due to any variation in some channels. A conventional EDFA would experience gain transients for the deletion or addition of one or more channels due to channel failure or burst traffic. These transients are reflected in the remaining channels, and may cause a substantial degradation in the system's bit-error rate. Transient effects, as well as gain fluctuation resulting in degradation of signal quality in the surviving channel, should be suppressed, and thus a gain clamping is required. This configuration is referred to as the GC–EDFA. The GC–EDFA is provided with a dynamic gain and flatness control arrangement that is fast enough to ensure reliable services continuously in the surviving channels, when one or more channels are suddenly dropped or added, as may be experienced when a system reconfiguration or fault interrupts some of the channels. The conventional EDFA, which is generally used in the transmission system, is subject to the characteristic definition that the input signal traffic is kept uniformly or constantly, and it is, therefore, unavailable for the burst packet-mode WDM optical switching system. We have demonstrated that the GC–EDFA comprising a double-pump laser diode (LD) and an electrical automatic gain controller (AGC) is available for the packet-mode optical switching system.

II. PROPOSED GC – EDFA

The problem of dynamic gain saturation dependent on the input power has been successfully overcome by using either

Contract grant sponsor: Korea Ministry of Information Communication Advanced Project